

THE PENNSYLVANIA STATE UNIVERSITY
SCHREYER HONORS COLLEGE

DEPARTMENT OF MATHEMATICS

THE NEURODYNAMICS OF BURSTING OSCILLATIONS IN THE HINDMARSH-ROSE
MODEL

STANLEY LEONARD TUZNIK
SPRING 2015

A thesis
submitted in partial fulfillment
of the requirements
for baccalaureate degrees
in Applied Mathematics and Physics
with honors in Applied Mathematics

Reviewed and approved* by the following:

Antonio Mastroberardino
Associate Professor of Mathematics
Thesis Supervisor

Joseph P. Previte
Associate Professor of Mathematics
Honors Adviser

*Signatures are on file in the Schreyer Honors College.

Abstract

The Hindmarsh-Rose model is a popular choice for simulating the behavior of a single neuron as it is able to capture, qualitatively, the spiking and bursting behaviors that are observed experimentally. This three-dimensional nonlinear system relies on a slow adaptation variable which dynamically switches the neuron from a period of firing to a quiescent period, a phenomenon known as bursting. We describe the underlying mechanism behind this bursting by reducing the model to a single-parameter system in the phase plane.

Table of Contents

List of Figures	iii
Acknowledgements	iv
1 Brief Introduction to Neurodynamics	1
1.1 The Physical Neuron and Bursting	2
1.2 The Hodgkin-Huxley Equations	3
2 Relaxation Oscillations	5
2.1 The Van der Pol Oscillator	6
2.1.1 History of the Relaxation Oscillator	6
2.1.2 Behavior and Analysis	7
2.2 The FitzHugh-Nagumo Model	10
2.2.1 Formulation	10
2.2.2 Behavior and Analysis	11
3 The Hindmarsh-Rose Model	14
3.1 Formulation	15
3.1.1 The 1982 Model	15
3.1.2 The 1984 Model	15
3.2 Analysis	17
3.2.1 Reduction	17
3.2.2 Bifurcations of Reduced Model	18
3.2.3 Hysteresis in the Reduced Model	24
3.2.4 The Full Model	25
3.3 Future Work	27
3.3.1 Chaotic Dynamics	27
3.3.2 Coupling	27
Bibliography	29

List of Figures

1.1	Neuron Diagram	3
2.1	Van der Pol Oscillator Trajectories	7
2.2	Van der Pol Oscillator Nullclines	9
2.3	FitzHugh-Nagumo Model Trajectories	11
2.4	FitzHugh-Nagumo Model Nullclines	12
3.1	Hindmarsh-Rose Trajectories	16
3.2	Hindmarsh-Rose Bifurcation Diagram (simple)	18
3.3	Stable Limit Cycle (I)	19
3.4	Saddle-Node Bifurcation (I)	20
3.5	Unstable Limit Cycle	20
3.6	Stable Limit Cycle (II)	21
3.7	Hopf Bifurcation	22
3.8	Saddle-Node Bifurcation (II)	22
3.9	Hindmarsh-Rose Bifurcation Diagram	23
3.10	Hysteresis Loop	24
3.11	Hindmarsh-Rose Phase Space	26
3.12	Chaotic Trajectory	27

Acknowledgements

I would like to thank my friends and family for their support through this writing at the culmination of my undergraduate career. Specifically, I thank my parents and Nicole for their unwavering love and support as I overthink everything that I do. Also, I would like to thank Dr. Antonio Mastroberardino for introducing me to this wonderful branch of applied mathematics and for giving me guidance and encouragement regarding both this thesis and my future in mathematics: it will always be very much appreciated.

Chapter 1

Brief Introduction to Neurodynamics

Mathematical neuroscience seeks to put the dynamical activity of the physical neuron on a rigorous mathematical foundation. The study of the structure and function of the central nervous system is a complex and strongly interdisciplinary effort, and involves an understanding of the basic structure of the neuron, a special type of biological cell. This chapter serves to introduce the physical neuron as well as an early single-neuron model, the Hodgkin-Huxley model. Some simpler models will be helpful to understand when discussing the more complicated Hindmarsh-Rose model for bursting oscillations, and analyses of these more basic models will be carried out in Chapter 2.

1.1 The Physical Neuron and Bursting

The neuron, the most basic element of the central nervous system, is a highly specialized cell. Located in the brain and spinal column, the neuron functions as a singular agent in a vastly interconnected network of similar nerve cells, and collectively these neurons are able to transmit signals as voltage (electric potential) spikes called *action potentials*. It is currently understood that the propagation of voltage signals across large networks of neurons gives rise to all observed brain function. Motivated by this belief, research in mathematical neuroscience attempts to apply a mathematical description to these systems.

Rather than trying to describe the activity of large ensembles of neurons, though, it would seem reasonable to consider first a single neuron. This problem of describing mathematically the various voltage activities of a single neuron has prompted much research in mathematical biology in the past sixty years. In fact, many mathematical models have been developed to emulate the physiological details of these singular nerve cells; indeed, just a basic understanding of the physical nature of the neuron has allowed for construction of some surprisingly accurate neural models (see Section 1.2). Several such models will be described in the following sections. We develop a fundamental understanding of the structure and function of the neuron.

The central focus of our work is the *neuron*, a specialized biological cell found throughout the central nervous system. While we could spend much time explaining the physiological intricacies of these nerve cells, we instead focus on the more relevant aspects of their anatomy.

There are many different types of neurons. In general, neurons have four main parts: the central cell body, the dendrites, the axon, and the nerve terminals [5]. A crude representation of a neuron is shown in Fig. 1.1. Here, the shaded area represents the cell body, containing the nucleus and other intracellular organelles. The dendrites, the branches nearest the nucleus, receive incoming signals from other neurons in the form of voltage pulses. The neuron's axon is the long branch down which outgoing signals propagate, and the nerve terminals communicate these pulses to other neurons. In the human central nervous system, massive numbers of neurons transmit voltage signals between one other, and these signals collectively allow the brain and body to function together. The study of neural networks is a broad subject that finds applications not only in neurobiology but also in data and computer science.

All neurons consist of and are immersed in aqueous chemical solutions consisting of many different kinds of ions, both positively and negatively charged. The cell membrane surrounds both the cell body and the axon and is the conductor along which the voltage signals travel. These pulses are transmitted as concentrations of various ions enter and exit the cell membrane through protein channels on the membrane surface. Many different types of ion channels exist with various proper-

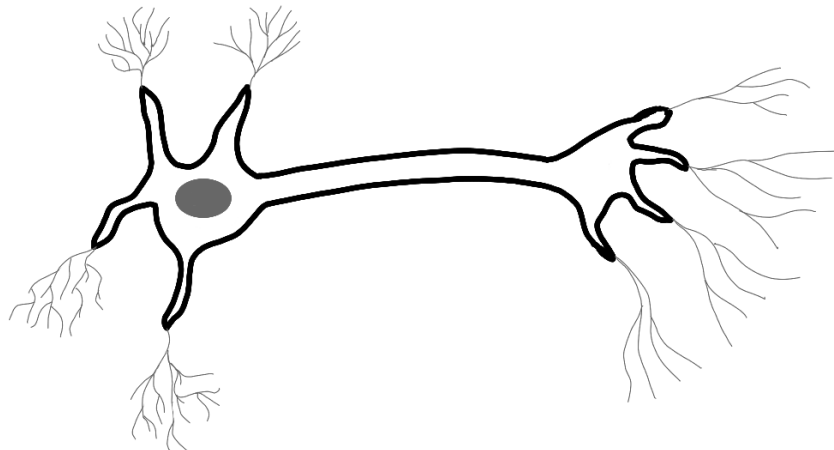


Figure 1.1: Diagram of a neuron (description in text).

ties: some are conductive to only a specific ion, for example. The voltage-dependent conductances of these various ion channels can give rise to different neural behaviors, and the modelling of a neuron with regard to the ion channels is a task often attempted alongside an experimental biologist. One of the most highly-regarded neural models, the Hodgkin-Huxley system, was designed as an electrical circuit with the ion channels represented as capacitors (see Section 1.2).

In this writing, we are interested in the behaviors that the membrane voltage of a neural model can exhibit. In all of the models considered here, a variable (x) represents this voltage. As time progresses, we can observe the trajectories that this voltage variable travels along. As one author points out, a “neuron is a dynamical system,” [12] and so we will apply mathematical ideas from dynamical systems theory to understand the details of these models. Specifically, most neural models describe the behavior of several variables, meant to represent the conductances of various ion channels, in the form of systems of differential equations. One of the most popular models is the Hodgkin-Huxley system, introduced in Section 1.2.

Two of the most common types of neural patterns are periodic spiking, in which voltage pulses repeat in infinite chains, and quiescence, in which the voltage equilibrates at some steady-state value and no spikes are observed. A third type of firing, considered in this paper, is *bursting*, a firing pattern in which regions of rapid spiking are separated by periods of quiescence. That is, spikes appear in bursts. This sort of behavior can be observed in several different types of neurons, including pancreatic beta cells [12]. We want to be able to understand how bursting can be simulated mathematically as a system of differential equations.

1.2 The Hodgkin-Huxley Equations

The system of equations developed by English biophysicists Alan Hodgkin and Andrew Huxley is widely regarded as the quintessential mathematical model of a single neuron [11]. Hodgkin and Huxley were awarded the Nobel Prize for Physiology or Medicine in 1963 for their development of this dynamical system in 1952. This model is unique amongst those in our discussion in that the

actual physiology of the neuron is considered. In particular, Hodgkin and Huxley realized that the ion channels in the neural membrane act as capacitors, and their model was developed in the same vein as that of an electrical circuit. The following subsections will outline the development of this system as well as describe its versatility as a simulator of single-neuron firing.

Dynamical systems is a natural language for describing the behavior of neurons [15]. As such, Hodgkin and Huxley sought to model the neuron as a dynamical system. In particular, they took the voltage-dependent conductances of the ion channels into account (see Section 1.1). By performing voltage-clamping experiments, they were able to measure the conductances of the various ions and fit them to particular functions. These functions were implemented in the model. Ultimately, the resultant model — known as a conductance-based model — is a benchmark in mathematical neuroscience, as it is able to demonstrate a wide and accurate variety of single-neuron behaviors.

This model is most often written as a four-dimensional system of differential equations:

$$\left\{ \begin{array}{l} c_M \frac{dV}{dt} = -\bar{g}_{\text{Na}} m^3 h (V - E_{\text{Na}}) - \bar{g}_{\text{K}} n^4 (V - E_{\text{K}}) - \bar{g}_{\text{L}} (V - E_{\text{L}}), \\ \frac{dn}{dt} = \phi [\alpha_n (V) (1 - n) - \beta_n (V) n], \\ \frac{dm}{dt} = \phi [\alpha_m (V) (1 - m) - \beta_m (V) m], \\ \frac{dh}{dt} = \phi [\alpha_h (V) (1 - h) - \beta_h (V) h], \end{array} \right. \quad \begin{array}{l} (1.1a) \\ (1.1b) \\ (1.1c) \\ (1.1d) \end{array}$$

where the variables m , n , and h represent the probabilities that various ion channels are open, the α_i and β_i are experimentally determined gating functions (unstated), the \bar{g} represent conductances of the channels, and ϕ is related to the temperature of the system [3].

This system is very complex. The equations are well-known for being able to accurately simulate many different types of neural behavior, including bursting. This is largely due to the fact that experimental data was used to construct the form of the equations. As a result of the system's complexity, it is difficult to analyze. It will be our goal in the rest of this paper to analyze a simpler system, the Hindmarsh-Rose model, which is known to demonstrate bursting trajectories. We hope to understand a simple mechanism by which bursting can be simulated.

Chapter 2

Relaxation Oscillations

The concept of a relaxation oscillation is ubiquitous in studies of nonlinear oscillations. In the first section of this chapter, we introduce the Van der Pol equation as a prime example of a single-state relaxation oscillator. In the subsequent section, we discuss the Fitzhugh-Nagumo system, a neuron model that adapts the Van der Pol oscillator to describe two stable states: a quiescent state and a periodically spiking state. Ultimately, we will observe in Chapter 3 how the Hindmarsh-Rose model was developed through adapting these relaxation oscillators to account for dynamic switching between states.

2.1 The Van der Pol Oscillator

As explained in the previous section, the Hodgkin-Huxley model — while very physiologically accurate — is quite cumbersome to analyze; in particular, it is a four-dimensional system of coupled equations, dependent upon multiple parameters. Oftentimes it is favorable to find a mathematically simple model that displays a specific behavior rather than analyze a complex model that displays a wide range of behaviors. The Fitzhugh-Nagumo and Hindmarsh-Rose models were developed in this manner. In fact, the two models share a foundation in the Van der Pol oscillator, the canonical example of what is known as a relaxation oscillator. In the following subsections, we trace the development of the Van der Pol equation and describe its behavior through a dynamical systems analysis. In particular, this model will serve as an introduction to basic dynamical mechanisms observed in the Hindmarsh-Rose model.

2.1.1 History of the Relaxation Oscillator

The advent of relaxation oscillations is most often attributed to one Balthasar Van der Pol, a Dutch physicist who is known for his work in radio waves. In 1926, he published a paper outlining his analysis of the voltage amplitude of a triode-driven circuit, in which appeared the dimensionless differential equation

$$x'' - \mu(1 - x^2)x' + x = 0 \quad (2.1)$$

where $\mu > 0$ is a parameter and x represents a voltage [1]. Upon analyzing this equation, Van der Pol stumbled upon an entirely new class of differential equations called relaxation oscillators [6]. Some trajectories of Eqn. 2.1 are shown for various values of μ in Fig. 2.1. From these trajectories, the nonlinear behavior of the oscillator is apparent: as μ is increased, the oscillations become less and less like the familiar simple harmonic motion that we observe in sinusoidal functions. The key characteristic of a relaxation oscillator is the sort of “build-up” behavior that they exhibit, similar to the periodic charging and discharging of a capacitor circuit.

Harkening back to the modelling of the neuron as an electrical circuit à la Hodgkin-Huxley (Section 1.2), it should not be surprising that the Van der Pol equation, developed to model a circuit, can be used to model a greatly simplified neuron. Indeed, the variable shown in Fig. 2.1 behaves qualitatively similar to the membrane voltage of a periodically spiking neuron, complete with variable time scales between spikes. As demonstrated by the representative trajectories in the figure, however, the Van der Pol oscillator is only capable of demonstrating infinite spike chains. That is, Eqn. 2.1 cannot be used to model a quiescent neuron or a bursting neuron, whose trajectories contain quiescent regions. To better understand why, we must conduct a dynamical systems analysis of the model.

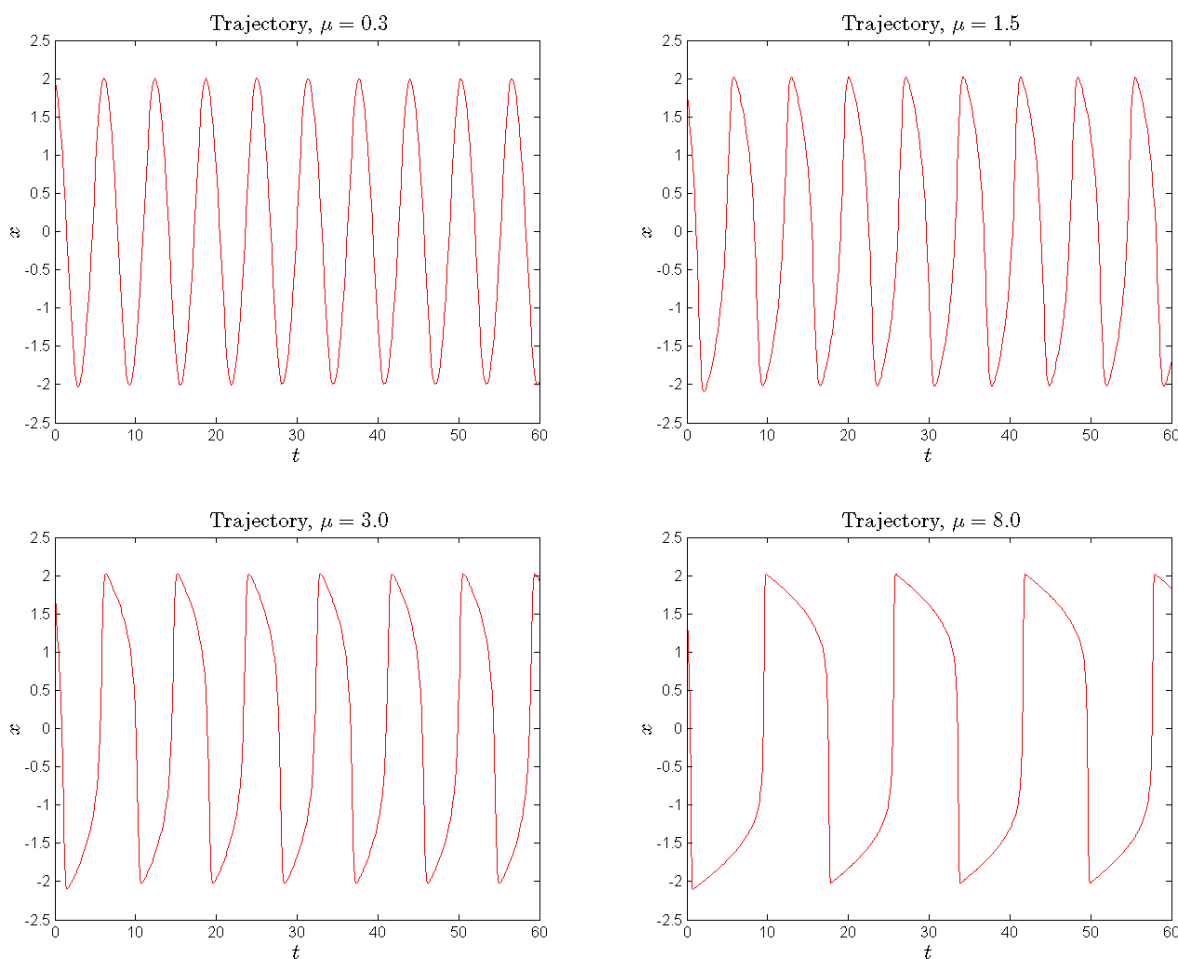


Figure 2.1: Trajectories for the Van der Pol oscillator. This system has a single behavior: infinite spiking. Note that the nonlinear aspect of the oscillator becomes more apparent as the parameter μ is increased.

2.1.2 Behavior and Analysis

Let us analyze this Van der Pol oscillator in the phase plane. The behavior that this particular relaxation oscillator offers will give us clues to understanding the behavior of the more complicated Hindmarsh-Rose oscillator. In particular, we wish to observe the specific mechanisms that generate the periodic spiking — the stable limit cycle¹ — of the Van der Pol equation:

$$\ddot{x} - \mu(1 - x^2)\dot{x} + x = 0, \quad \mu > 0 \quad (2.2)$$

This is a second-order nonlinear ordinary differential equation. Note that there are at least two interesting limiting cases. First, as μ tends toward zero, the equation reduces to the simple harmonic oscillator. Thus, μ can be thought of as controlling the strength of the system's nonlinear damping.

¹Limit cycles are isolated, periodic trajectories of a dynamical system. Proving the existence of a limit cycle is not a trivial matter, in general.

Second, the quadratic term in x can be neglected for very small x , resulting in an oscillator subject to linear damping with coefficient μ .

A dynamical systems analysis of the model for general μ involves the reduction of the second-order equation to a system of two coupled first-order equations. Most often, this transformation is achieved through a simple substitution, $y \equiv \dot{x}$, resulting in the system:

$$\begin{cases} \dot{x} = y, & (2.3a) \\ \dot{y} = -x + \mu(1 - x^2)y, & (2.3b) \end{cases}$$

Now, the state of our dynamical system is entirely defined by the state variables (x, y) . Analysis of such a system begins by considering the *nullclines*, curves along which the flow in one direction is zero. Appropriately, we find nullclines by setting $\dot{x} = 0$ and $\dot{y} = 0$. From the above coupled equations, the nullclines are

$$\dot{x} = 0 \Rightarrow y = 0, \quad (2.4a)$$

$$\dot{y} = 0 \Rightarrow y = \frac{x}{\mu(1 - x^2)} \quad (2.4b)$$

It should be clear that the points of intersection of these nullclines are the fixed (or equilibrium) points of the system. These fixed points can be thought of as constant or steady-state solutions to the system of differential equations. Typically, we would proceed to determine the fixed points, plot the nullclines, and attempt to observe limit cycles.

For this system, however, there is an alternate definition of the y -variable that better simplifies the graphical analysis [14]. Note that the left-hand side of Eqn. 2.2 can be rewritten using basic differentiation rules:

$$\frac{d}{dt} \left[\frac{1}{\mu} \dot{x} - x + \frac{1}{3} x^3 \right] + \frac{1}{\mu} x = 0 \quad (2.5)$$

Now, let $y \equiv x - \frac{1}{3}x^3 - \frac{1}{\mu}\dot{x}$. The previous equation becomes

$$-\dot{y} + \frac{1}{\mu}x = 0 \quad (2.6)$$

giving a new two-dimensional system:

$$\begin{cases} \dot{x} = \mu \left(x - \frac{1}{3}x^3 - y \right), & (2.7a) \\ \dot{y} = \frac{1}{\mu}x, & (2.7b) \end{cases}$$

We are ready to analyze this system. Setting \dot{x} and \dot{y} to zero, the nullclines are

$$\dot{x} = 0 \Rightarrow y = x - \frac{1}{3}x^3, \quad (2.8a)$$

$$\dot{y} = 0 \Rightarrow x = 0, \quad (2.8b)$$

The advantage of using this choice of variables is obvious: both nullclines are independent of the parameter, μ , while the y -nullcline is simply the y -axis. That is, any flow across the y -axis is purely

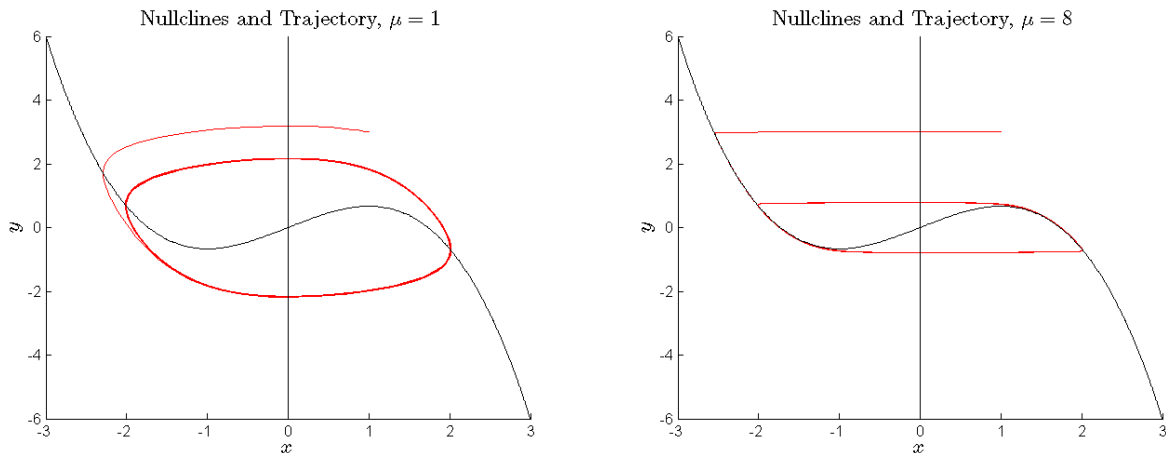


Figure 2.2: Nullclines and trajectories for the Van der Pol oscillator. As μ is increased, the oscillator becomes more nonlinear and the trajectory “hugs” the cubic nullcline. The proximity of the trajectory to the nullcline gives rise to the variable time scales during a cycle of the oscillation.

in the x -direction. The cubic x -nullcline, along which $\dot{x} = 0$, is more interesting, and ultimately determines the form of the limit cycle. These lines are plotted in Fig. 2.2. Note that the origin is the only fixed point for this system and that its existence is independent of the parameter μ .

We are interested in determining criteria for the stability of the equilibrium at the origin. As usual, we construct the Jacobian matrix to linearize about this fixed point²:

$$J(\bar{x}, \bar{y}) = \begin{bmatrix} \mu(1 - \bar{x}^2) & -\mu \\ \frac{1}{\mu} & 0 \end{bmatrix}$$

where (\bar{x}, \bar{y}) represents a fixed point of the system. The eigenvalues of this Jacobian evaluated at $(\bar{x}, \bar{y}) = (0, 0)$ are

$$\lambda_{1,2} = \frac{1}{2} \left(\mu \pm \sqrt{\mu^2 - 4} \right)$$

Since the formulation of the Van der Pol equation restricts the parameter μ to be strictly positive, the real parts of the eigenvalues are positive for any μ . Thus, the equilibrium at the origin is unstable. Precisely, the origin is an unstable spiral for $0 < \mu < 2$ and is an unstable node for $2 \leq \mu < \infty$.

Note from Fig. 2.2 that we appear to yet have some stable structure in this system despite the instability of the single equilibrium. Specifically, initial conditions are globally attracted to a stable limit cycle which surrounds the unstable equilibrium at the origin. The existence of this limit cycle can actually be proven through an application of Lienard’s theorem [14]. The nullclines define the shape of the trajectories in the phase plane: trajectories close to the nullclines will move slowly, since the flow in one direction is close to zero. Here, the nullclines are unaffected by changes in the parameter, through our particular choice of variable y .

²The use of the Jacobian matrix and its eigenvalues to determine local stability of fixed points can be thought of as a compact way of representing a multivariable Taylor expansion. This method is introduced more fully by Strogatz [14].

The salient points of this Van der Pol example are the physiological interpretations of the dynamical behavior. Recall that x -variable represents the voltage of an electronic system (the membrane voltage of the neuron) and the y -variable is related to the time derivative of this voltage. Thus, stable fixed points of a neural model represent quiescent (nonfiring) states, and stable limit cycles correspond to periodic firing states [12]. In the case of the Van der Pol equation, only the stable limit cycle behavior is achieved. That is, there is no range of parameter values that admit a stable fixed point. In our goal of simulating bursting behavior, we need to find a model that exhibits both stable fixed points and stable limit cycles. The FitzHugh-Nagumo model, discussed in the next section, is a step in the right direction.

2.2 The FitzHugh-Nagumo Model

We have seen that the early Van der Pol model is able to simulate very simplistic neurons with only a single behavior: periodic spiking. As far as bursting is concerned, this model is unsatisfactory since it is unable to display any quiescent states. This is a result of there existing no bifurcations as the system's single parameter is varied. In this section, we describe the FitzHugh-Nagumo model, a single-neuron model that improves on the Van der Pol oscillator by admitting the existence of quiescent states as well as periodic spiking states. Specifically, we can have either a stable fixed point or a stable limit cycle in the FitzHugh-Nagumo system. Additionally, we will observe a particular bifurcation, the Hopf bifurcation, which will play a key role in the development of the Hindmarsh-Rose model, later.

2.2.1 Formulation

This next model was published by Richard FitzHugh in 1961 as a modified Van der Pol oscillator which the author refers to as the ‘‘Bonhoeffer-Van der Pol’’ model [4]. The author sought a simpler form of the Hodgkin-Huxley formulation (Section 1.2) that was more realistic than the Van der Pol oscillator. As in the creation of the Hodgkin-Huxley model, a conceptualization of the neuron membrane as a circuit was used to develop the model: Nagumo designed the equivalent circuit for this model, and shares the name with FitzHugh. The system is usually written as

$$\begin{cases} \dot{x} = c \left(y + x - \frac{1}{3}x^3 + I \right), & (2.9a) \\ \dot{y} = -\frac{1}{c} (x - a + by), & (2.9b) \end{cases}$$

where a , b , c , and I are parameters with the conditions

$$1 - 2b/3 < a < 1, \quad 0 < b < 1, \quad b < c^2$$

for reasons we will soon see.

In a study of this model, we typically fix a , b , and c and let I vary as our parameter of interest. Through our analysis in the next subsection, we will see that the FitzHugh-Nagumo equations exhibit two stable states separated by a bifurcation. This bifurcation can be thought of as being brought on by an applied current — the parameter I — being moved beyond a threshold level. Rather than delve into the historical details of the formulation of this model, we provide the justification for the choice of the form of the equations through a dynamical systems analysis.

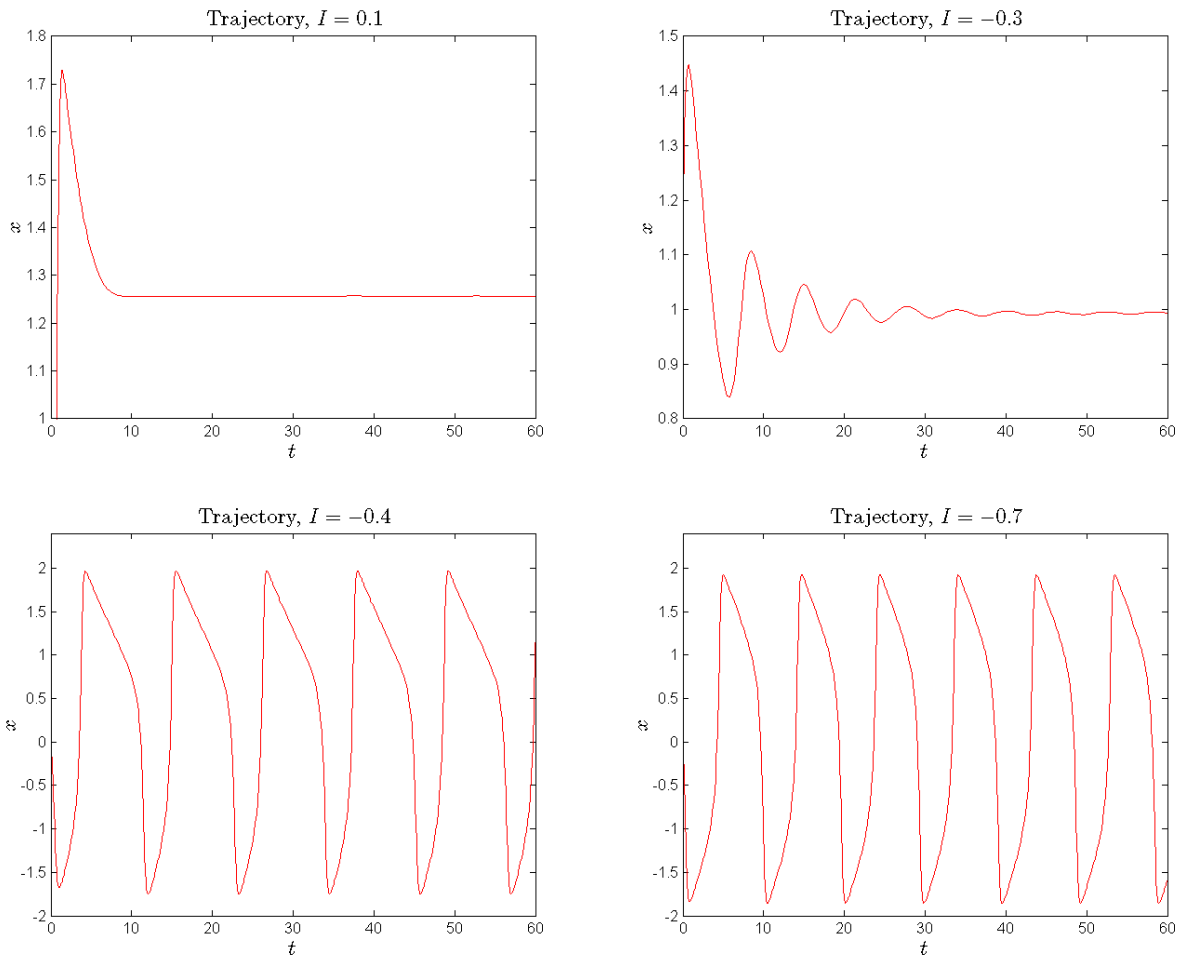


Figure 2.3: Trajectories for the FitzHugh-Nagumo system. There are two general types of behavior for this system: a quiescent steady state (top) and an infinitely spiking state (bottom). Note the nonlinear character of the oscillations.

2.2.2 Behavior and Analysis

As in the case with the Van der Pol oscillator, we will analyze the FitzHugh-Nagumo system in the phase plane. The nullclines of Eqns. 2.9 are

$$\dot{x} = 0 \quad \Rightarrow \quad y = \frac{1}{3}x^3 - x - I, \quad (2.10a)$$

$$\dot{y} = 0 \quad \Rightarrow \quad y = \frac{1}{b}(a - x), \quad (2.10b)$$

As expected from the formulation of the FitzHugh-Nagumo system as a modified Van der Pol system, we retain the cubic x -nullcline and the linear y -nullcline. This time, however, the values of the system parameters do affect the nullclines. Specifically, the injected current parameter, I , serves to shift the x -nullcline parallel to the y -axis. This will shift the point of intersection of the nullclines (the fixed point) along the cubic nullcline. Recall the conditions imposed on the

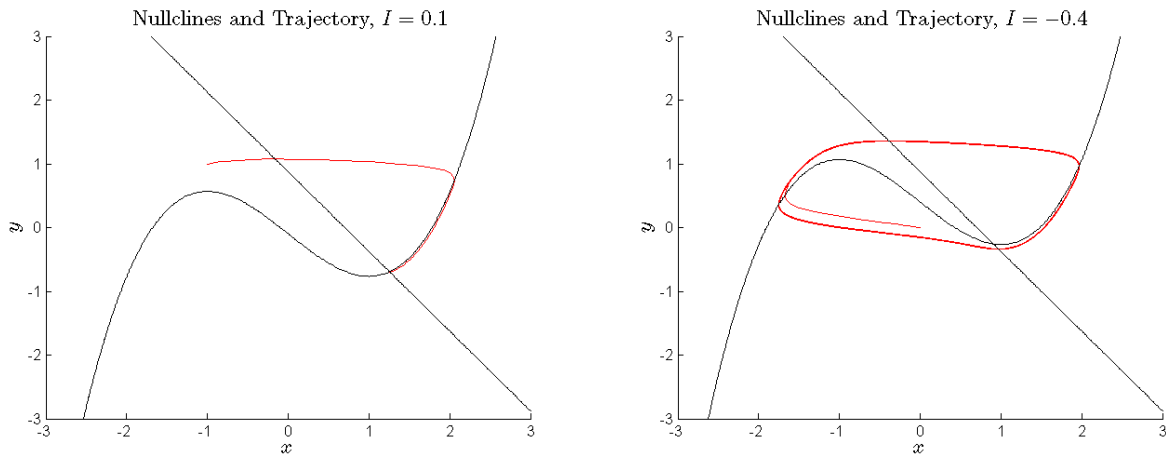


Figure 2.4: Nullclines and trajectories for the FitzHugh-Nagumo model. For some values of I (left), there exists a single stable fixed point. For other values of I (right), the fixed point is unstable and is surrounded by a stable limit cycle. Varying I amounts to shifting the cubic nullcline.

parameters:

$$1 - 2b/3 < a < 1, \quad 0 < b < 1, \quad b < c^2$$

These restrictions force the two nullclines to intersect at only a single point. In particular, we choose the standard values $a = 0.7$, $b = 0.8$, and $c = 3$, and we let I be our parameter of interest. This suits our interpretation of I as an injected current, a parameter which could be experimentally controlled. The nullclines are plotted for two different values of I in Fig. 2.10, along with trajectories for those parameter values. Note that for $I = 0.1$ the equilibrium is a stable node, but for $I = -0.4$ it is unstable, surrounded by a familiar-looking limit cycle. We can locate bifurcations through the same linear stability analysis that we applied in the Van der Pol case. First, we find an equation for the equilibrium points of the system. By equating the nullclines (eliminating y), we obtain

$$\bar{x}^3 + \frac{3}{4}\bar{x} - 3\left(I + \frac{7}{8}\right) = 0 \quad (2.11)$$

with our particular parameter values. That is, the equilibrium points \bar{x} satisfy this implicit cubic equation for each I , generating a continuum of equilibria (the corresponding \bar{y} can be computed from either of the nullclines). We now have a handle on all of the possible fixed points of this system in terms of our parameter of interest, I . Next, we want to consider the stability of these equilibria.

As usual, we construct the Jacobian matrix for the system:

$$J(\bar{x}, \bar{y}) = \begin{bmatrix} 3(1 - \bar{x}^2) & 3 \\ -\frac{1}{3} & -\frac{4}{15} \end{bmatrix}$$

Instead of solving the matrix equation $|J(\bar{x}, \bar{y}) - \lambda I| = 0$ for the eigenvalues, λ_1 and λ_2 , which can be quite complicated, we use the shortcut for 2×2 matrices:

$$\lambda_{1,2} = \frac{1}{2} \left(\text{Tr}(J(\bar{x}, \bar{y})) \pm \sqrt{\text{Tr}(J(\bar{x}, \bar{y}))^2 - 4\Delta(J(\bar{x}, \bar{y}))} \right)$$

where $\text{Tr}(J)$ and $\Delta(J)$ represent the trace and determinant of J , respectively. Recall that a fixed point is stable if the real part of both eigenvalues is negative, and it will be a focus if the eigenvalues are complex. Instead of conducting the entire stability analysis, we seek a particular bifurcation.

From the trajectories shown in Fig. 2.3, we see that we have a limit cycle for some values of I and no limit cycle for others. It turns out that the appearance of a limit cycle about a fixed point can occur at what is called a *Hopf bifurcation* [3] [12]. These bifurcations occur when two complex-conjugate eigenvalue pairs cross the imaginary axis, that is, when $\text{Re}(\lambda_1) = \text{Re}(\lambda_2) = 0$, simultaneously, but $\text{Im}(\lambda_1) \neq 0$, $\text{Im}(\lambda_2) \neq 0$. In our case, this can potentially occur when $\text{Tr}(J) = 0$:

$$\bar{x}_H = \pm \sqrt{1 - \frac{4}{45}} = \pm 0.955$$

Using Eqn. 2.11 to find the corresponding parameter values for these possible bifurcation points, we find two Hopf bifurcations:

$$(\bar{x}_H, I_H) = (0.955, -0.346) \quad \text{and} \quad (\bar{x}_H, I_H) = (-0.955, -1.404)$$

The bifurcation observed between the two plots in Fig. 2.10 is obviously the Hopf bifurcation corresponding to $I_H = -0.346$.

Recall that the Van der Pol oscillator was only able to exhibit infinitely spiking trajectories, since its equations displayed no bifurcations. In the FitzHugh-Nagumo model, the Hopf bifurcations that we just located serve to switch the limit cycles on and off. For injected current $I < -1.404$ and $I > -0.346$ we have a stable fixed point, representing a quiescent neuron; for $-1.404 < I < -0.346$ we have a stable limit cycle, or periodic firing. It seems as if this Hopf bifurcation is the missing key to our puzzle.

However, one issue renders the FitzHugh-Nagumo system ultimately unfit to model bursting neurons: the switching behavior (bifurcations) occur only when a parameter is changed, not as the system evolves in time. That is, the FitzHugh-Nagumo system can only display one of two possible states at a time, quiescence or periodic spiking, and is unable to dynamically switch between the two. For bursting to occur, we need a model that is able to switch between states as time progresses, without an experimentalist tweaking the parameters. The Hindmarsh-Rose model, discussed in the next chapter, resolves this issue.

Chapter 3

The Hindmarsh-Rose Model

In Chapter 1, we mentioned that some specific neurons are known to display bursting behavior. In Chapter 2, we discussed two models that were not able to demonstrate bursting dynamics. In this chapter, we explain how bursts can be described mathematically and we focus on the development of the Hindmarsh-Rose model for single-neuron bursting. In Section 3.2, we carry out an analysis of this model and demonstrate that the switching between resting and firing states is a result of hysteresis in the model's bifurcation diagram.

3.1 Formulation

The Hindmarsh-Rose model that we analyze here was developed as a modified FitzHugh-Nagumo model. In this section we describe development of the Hindmarsh-Rose model as a departure from FitzHugh-Nagumo.

3.1.1 The 1982 Model

The first version of the Hindmarsh-Rose model was put forth in 1982 [8]. The model was a two-dimensional system, developed not to simulate bursting but instead the lengthy interspike interval common to many periodic spiking patterns. Specifically, Hindmarsh and Rose aimed to improve upon the FitzHugh-Nagumo model in this regard, and so their equations (not stated here) attempt to generalize the FitzHugh-Nagumo equations. These equations are quite complex, however: they contain cubic polynomials as well as exponential functions in the two variables. In fact, the precise forms of these equations come from fitting experimental data recorded by Hindmarsh and Rose, and so it is hardly surprising that this model simulates the actual interspike interval well. As this model does not demonstrate bursting behavior, we do not analyze it here.

3.1.2 The 1984 Model

In 1984, Hindmarsh and Rose published a modified version of their 1982 model [9]. This new system, henceforth referred to as the Hindmarsh-Rose model, was developed to simulate bursting [7]. This model is a three-dimensional system:

$$\begin{cases} \dot{x} = y - ax^3 + bx^2 + I - z, & (3.1a) \\ \dot{y} = c - dx^2 - y, & (3.1b) \\ \dot{z} = r(s(x - x_1) - z), & (3.1c) \end{cases}$$

Plotted in Fig. 3.1 are some trajectories of this system for various parameters values. Clearly, the model exhibits the desired bursting behavior. Note that the bursts are periodic now, whereas the other models were only able to achieve periodic spikes without quiescent regimes. Additionally, by tweaking the parameters we can obtain bursts with different frequencies and numbers of spikes, making this model more widely applicable for simulating different types of neurons.

We will introduce this system in contrast with the previously discussed FitzHugh-Nagumo model (see Section 2.2). First, note that the \dot{x} equation is still cubic in x but has replaced the x term of FitzHugh-Nagumo with an x^2 term. The equation retains the parameter I from FitzHugh-Nagumo, but, more interestingly, also contains a linear term in z , the system's third variable. Thus,

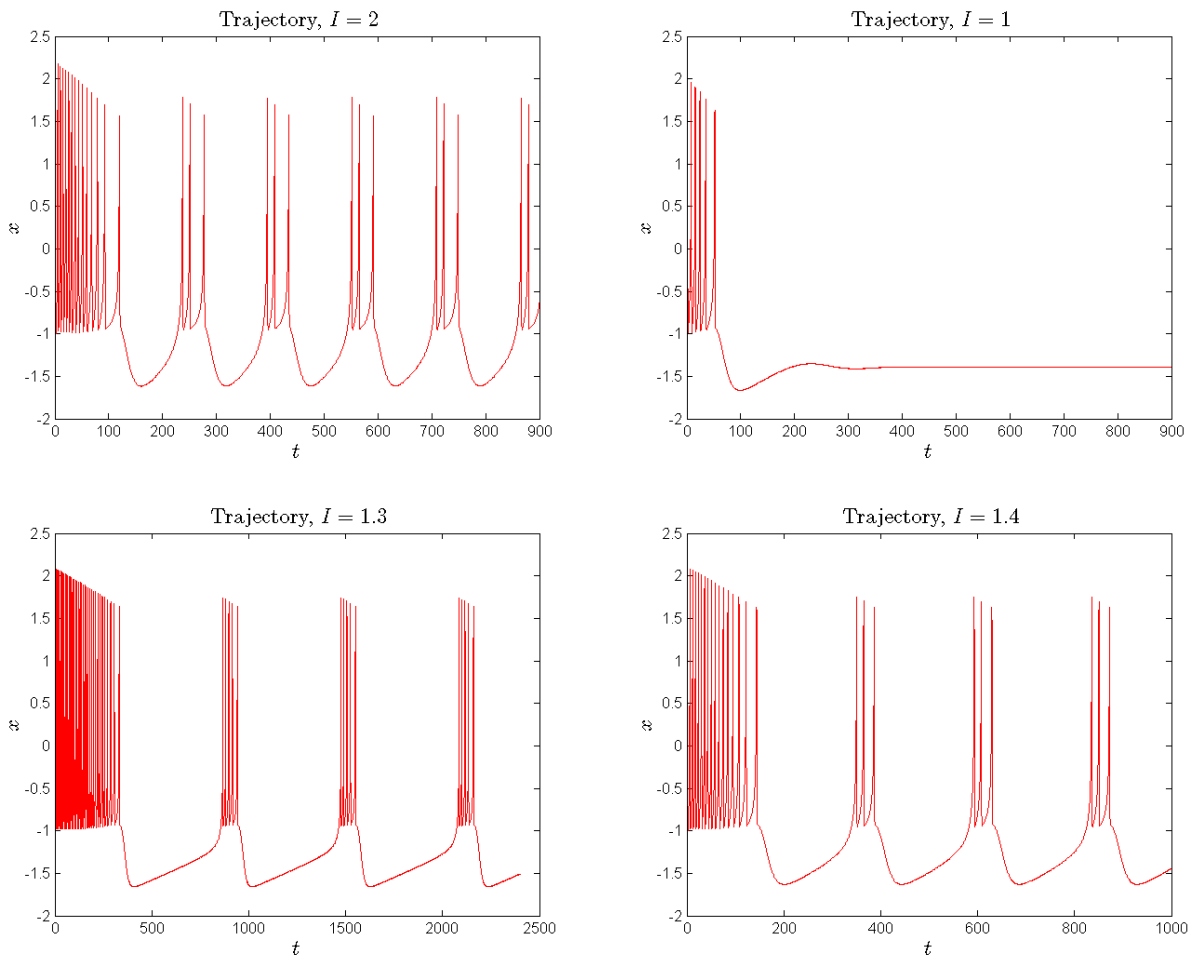


Figure 3.1: Trajectories for the three-dimensional Hindmarsh-Rose system. Note the variety of attainable behaviour: quiescence as well as bursting with varying frequencies and numbers of spikes.

the z variable decreases the membrane potential.

The \dot{y} equation is unchanged from the FitzHugh-Nagumo model apart from the replacement of the linear x term with a quadratic x term. This will turn out to be a crucial change; recall that the x - and y -nullclines of FitzHugh-Nagumo were cubic and linear in x , respectively. Now, the y -nullsurface¹ will be quadratic in x — the existence of multiple fixed points is possible.

Lastly, the \dot{z} equation and z variable are entirely new. Hindmarsh and Rose offer the following physiological interpretation of the variables: x represents membrane voltage, y represents a recovery variable (for individual spikes), and z represents a slow adaptation current that serves to switch bursts on and off [9]. We wish to determine the exact mechanism by which this switching occurs.

Before attempting our analysis, let us briefly consider the parameters of this model. Note that we have a total of eight parameters: a , b , c , d , r , s , x_1 , and I . The a , b , c , and d parameters be-

¹The nullclines are replaced with surfaces because we are in three-dimensional phase space. For example, setting $\dot{x} = 0$ will result in the obtaining of the equation of some surface in y and z , for example.

have as in previous models, strengthening or weakening the effects of various terms in the x and y equations; we generally fix these as constants. The parameter x_1 is related to the coordinates of the fixed point of the system without the adaptation variable, z , and is universally fixed as $x_1 = -8/5$.

The parameters of utmost interest are r and I . Here, note that r multiplies the entire \dot{z} equation. In accordance with our above-mentioned notion of z as a *slow* current, we usually choose r to be very small so that z changes slowly in time. During our analysis, we shall see how this assumption can be used to justify a simplification of the model. Lastly, the I parameter represents an applied current, as in the FitzHugh-Nagumo model. As before, we are interested in how the Hindmarsh-Rose model behaves as the applied current, an experimentally controlled parameter, changes.

3.2 Analysis

In this section, we analyze the Hindmarsh-Rose model of 1984. In particular, we are interested in observing how bursting can be achieved in this model. Earlier models, like FitzHugh-Nagumo, exhibit two states: firing and quiescence. These models cannot dynamically switch between these states, however, and thus are not good for simulating bursting. The Hindmarsh-Rose model, however, is able to attain some sort of switching dynamics through the change of the y -nullcline to a quadratic function in x . The model is stated again:

$$\begin{cases} \dot{x} &= y - ax^3 + bx^2 + I - z, \\ \dot{y} &= c - dx^2 - y, \\ \dot{z} &= r(s(x - x_1) - z), \end{cases}$$

As discussed in the previous section, this model is algebraically similar to the FitzHugh-Nagumo model, but with some necessary changes. Specifically, the inclusion of a third state variable, z , makes the system slightly more difficult to analyze, as we now have a system of three variables and eight parameters. Much work has been recently done in characterizing the different behaviors of this system under various parameter sweeps [13]. In this work, we take a more general approach. To simplify our analysis, we reduce the three-dimensional system — which we henceforth refer to as the “full” model — to a two-dimensional reduced system which we can analyze in the plane.

3.2.1 Reduction

Recall from the previous section that the parameter r is usually very small relative to the other parameters and variables, typically on the order of $1/1000$. Since this r is the coefficient of the time derivative of z ,

$$\dot{z} = r(s(x - x_1) - z)$$

r can be thought of as controlling the rate of change of z . That is, a small r corresponds to z changing very slowly in time. For small time scales, we can justify the approximation

$$\dot{z} \approx 0$$

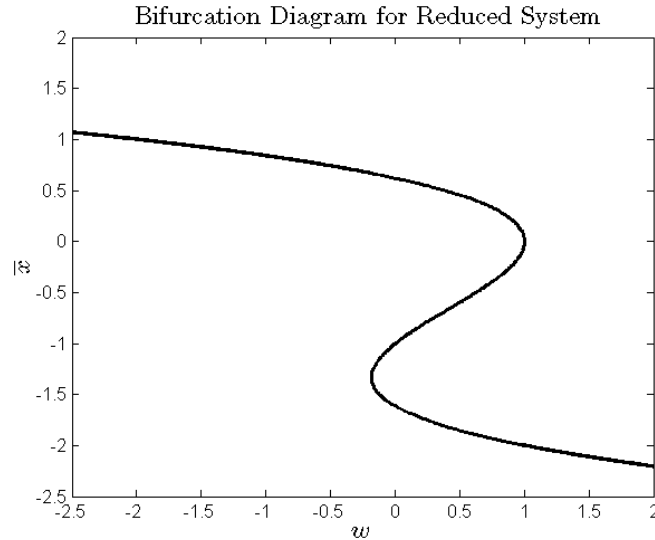


Figure 3.2: Simple bifurcation diagram for the reduced Hindmarsh-Rose model. There exist three primary regions: two regions (left, right) where a single fixed point exists and a region (center) with three fixed points coexisting.

We will treat z as a *slow parameter* and observe bifurcations in the reduced model as we vary z . More precisely, we define the parameter w as

$$w \equiv -(I - z)$$

where we subsume I into w along with z , for simplification. Finally, we will fix the remaining parameters such that the full model would exhibit a bursting trajectory: $a = 1$, $b = 3$, $c = 1$, and $d = 5$. We have reduced the full model to a two-dimensional, one-parameter system:

$$\begin{cases} \dot{x} = y - x^3 + 3x^2 - w, \\ \dot{y} = 1 - 5x^2 - y, \end{cases}$$

We hope that an analysis of this reduced model will give us clues as to the behavior of the full, three-dimensional model.

3.2.2 Bifurcations of Reduced Model

As usual, we first consider the nullclines of this reduced model:

$$\dot{x} = 0 \quad \Rightarrow \quad y = x^3 - 3x^2 + w, \tag{3.2a}$$

$$\dot{y} = 0 \quad \Rightarrow \quad y = 1 - 5x^2, \tag{3.2b}$$

As compared with the nullclines of the FitzHugh-Nagumo equations, there are important differences. The x -nullcline is still cubic in x , and is now shifted by the parameter w . The y -nullcline is quadratic in x , where it was previously linear in x for the FitzHugh-Nagumo equations. This difference will turn out to be crucial, as it serves to create additional fixed points that are absent

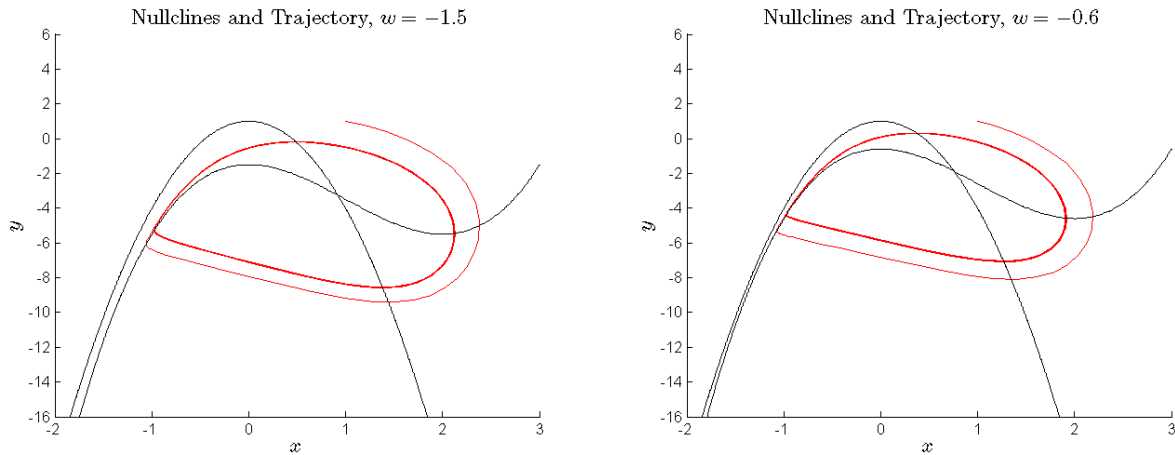


Figure 3.3: Nullclines and trajectories for the Hindmarsh-Rose model. Notice that the nullclines draw closer together as the parameter w is increased. A stable limit cycle exists about the system's single, unstable fixed point.

from FitzHugh-Nagumo.

We can identify the fixed points of this system by solving Eqns. 3.2:

$$\bar{x}^3 + 2\bar{x}^2 + (w - 1) = 0$$

where \bar{x} represents the x -coordinate of a fixed point of the system. This equation is plotted as a bifurcation diagram in Fig. 3.2. Notice that the system has a single fixed point for some ranges of w and three fixed points for different w . The bifurcations that take the system between these two states will prove to account for the observation of bursting behavior. To locate these and other bifurcations and to understand how the bursting dynamics occur in the full model, we pick various values of w and label bifurcations in Fig. 3.2.

We start with some negative values for w . Plotted in Fig. 3.3 are the nullclines and several trajectories for $w = -1.5$ and $w = -0.6$. First, notice that the single fixed point, where the nullclines intersect, is unstable and is surrounded by a stable limit cycle, corresponding to a periodic spiking state, as in the FitzHugh-Nagumo model (Chapter 2). As predicted from the algebraic form of the system, increasing w shifts the cubic nullcline upward parallel to the y -axis, creating a “narrow channel” between the leftmost branches of the nullclines [9]. Recalling that nullclines are curves along which the flow in one direction is zero, we are not surprised to see that trajectories move more slowly inside this channel as the nullclines draw closer together. This channel-narrowing allows the model to display a larger variety of interspike intervals – for periodic spiking, the model can simulate many different frequencies.

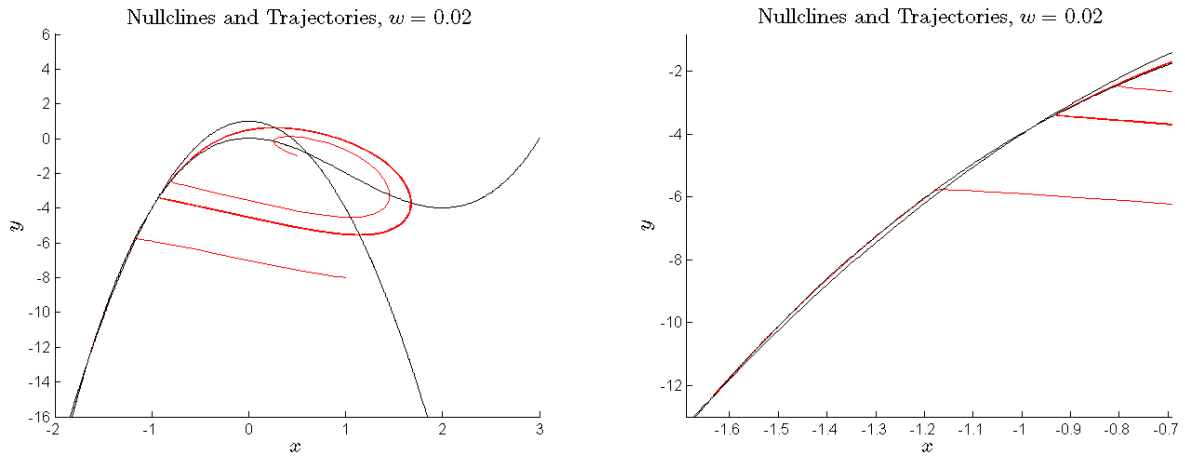


Figure 3.4: A saddle-node bifurcation has occurred. The nullclines have intersected, created two additional fixed points (inset on right).

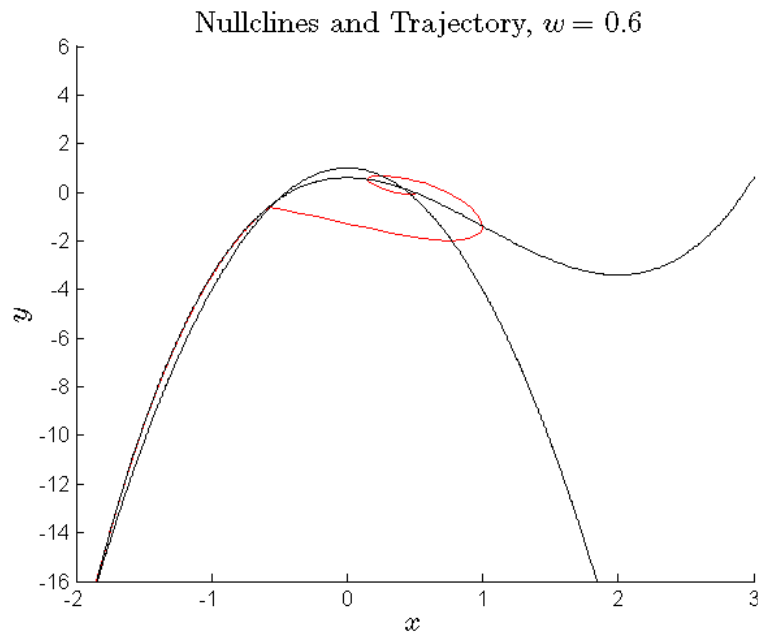


Figure 3.5: A homoclinic bifurcation has occurred, and the limit cycle has been destabilized. Only the leftmost fixed point is stable.

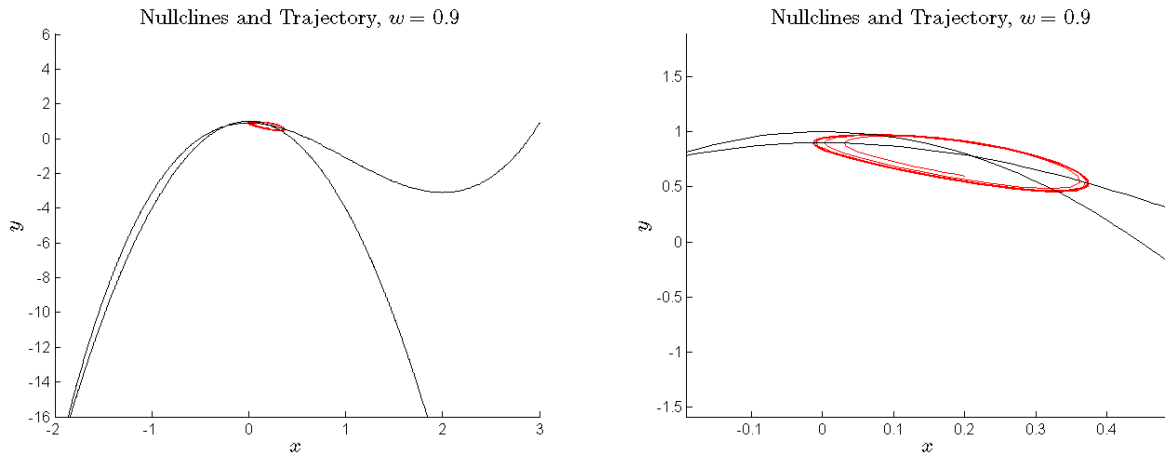


Figure 3.6: A second homoclinic bifurcation has occurred, and the limit cycle has restabilized.

As we continue to increase w , the nullclines draw ever closer together. Eventually, the nullclines intersect, at first tangentially, creating a single fixed point which immediately branches into two new fixed points. This is a *saddle-node bifurcation*, and it corresponds to a transition from the leftmost single-fixed point regime to the three-fixed point regime in Fig. 3.2.

From the trajectories in Fig. 3.4, we can infer the stabilities of the three fixed points. The rightmost fixed point retains its instability, and is still surrounded by a stable limit cycle. The central fixed point is unstable, since trajectories starting near it either tend toward the limit cycle or toward the final, leftmost fixed point. Thus, the leftmost fixed point is stable. Note that we have two stable structures, now: a stable fixed point and a stable limit cycle. This bistability indicates that the Hindmarsh-Rose model is capable of simulating both quiescent behavior and periodic spiking for the same value of the parameter I , a feat which the FitzHugh-Nagumo model was unable to achieve.

We increase I further. As the cubic nullcline moves further upward, the central fixed point is drawn up along the nullclines toward the stable limit cycle. Eventually, this unstable fixed point collides with the stable limit cycle in what is called a *homoclinic bifurcation*, destabilizing the limit cycle. After this bifurcation, all initial conditions tend toward the leftmost stable fixed point, though some take a short excursion around the destabilized limit cycle, as shown in Fig. 3.5. For these parameter values, there exists only a quiescent state.

As we continue to increase I , we continue to shift the cubic nullcline upward. The lower branch of the unstable limit cycle also shifts upward, approaching the central unstable fixed point again, as in Fig. 3.5. Eventually, the two unstable objects collide in what is a reversal of the earlier homoclinic bifurcation: the limit cycle is restabilized. However, the amplitude of the re-stabilized limit cycle is quite small, and closely surrounds the rightmost unstable fixed point, as seen in Fig. 3.6.

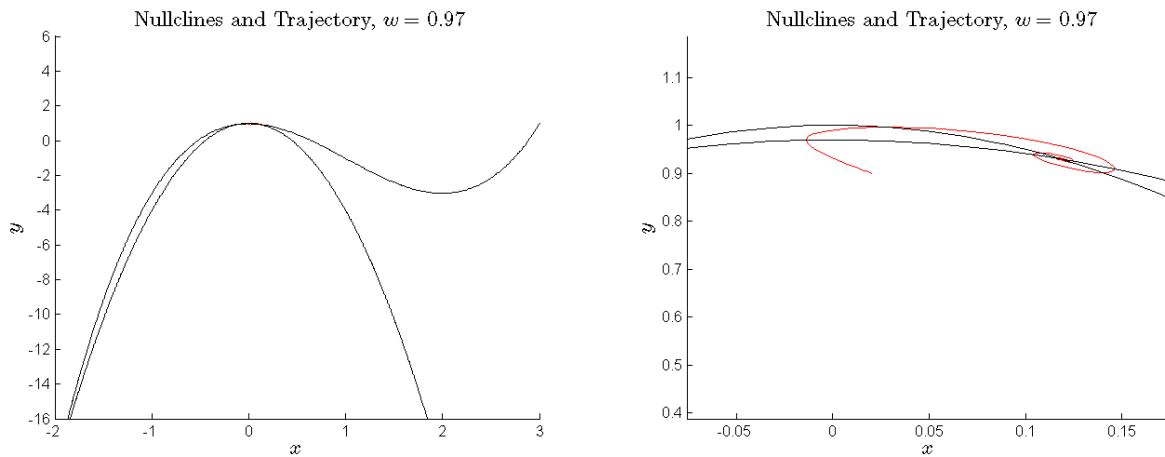


Figure 3.7: A Hopf bifurcation has occurred. The stable limit cycle has tightened about the unstable fixed point inside of it. As the two collide, the fixed point is stabilized and the limit cycle annihilated.

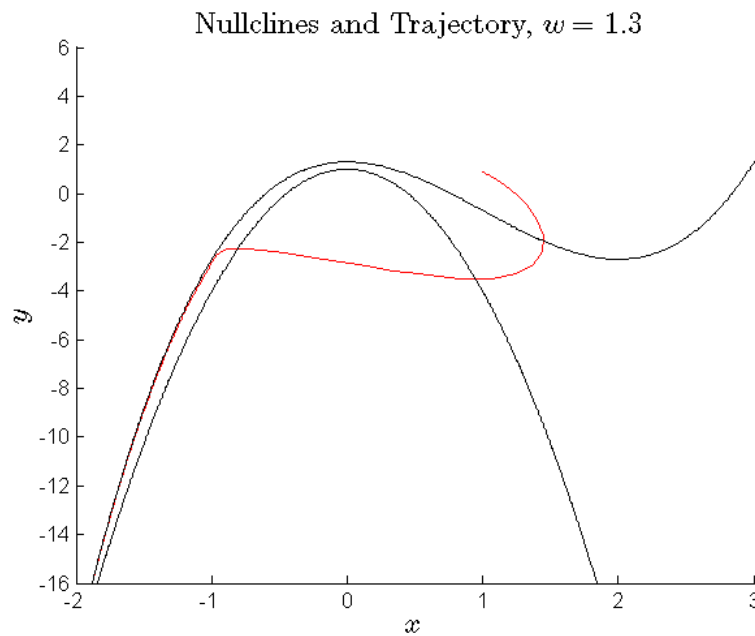


Figure 3.8: Finally, another saddle-node bifurcation has occurred. The nullclines have shifted enough to destroy two fixed points, and the system is left with a single stable structure, a fixed point.

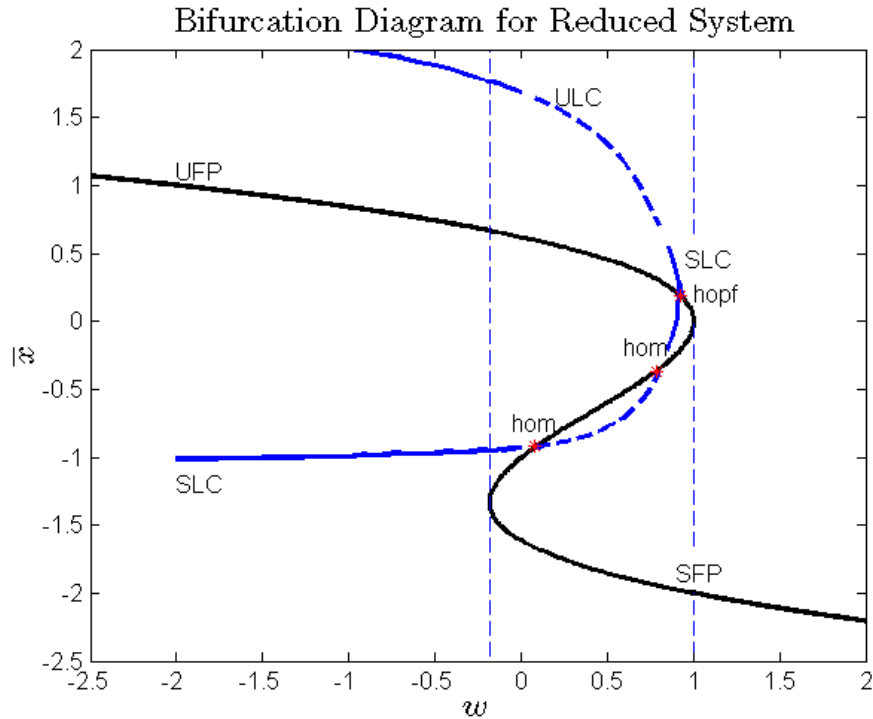


Figure 3.9: Fully-labeled bifurcation diagram for the reduced Hindmarsh-Rose model. The solid (dashed) blue lines represent the maxima and minima of the stable (unstable) limit cycles.

Increasing the parameter further shrinks the limit cycle around the fixed point. Eventually, this limit cycle collides with the fixed point, annihilating the limit cycle and stabilizing the fixed point through a Hopf bifurcation, as seen in the FitzHugh-Nagumo model. The aftermath is shown in Fig. 3.7. Again, we have bistability. At this point, the central fixed point is unstable while the remaining two fixed points are stable. All periodic behavior is gone, and we are left with two possible quiescent states.

Increasing the parameter further, we shift the cubic nullcline enough to encounter the final bifurcation: another saddle-node bifurcation. The cubic nullcline is instantaneously tangential to the quadratic nullcline, and then the two rightmost fixed points are destroyed. A single fixed point remains, and is stable, as shown in Fig. 3.8. Any further increase of I slightly shifts this fixed point. We have only a single, quiescent state.

This concludes our exploration of the various bifurcations of this model. The complete and labelled bifurcation diagram is depicted in Fig. 3.9. Of course, we have only considered a small range of the possible values for the parameter I . However, we claim that the dynamics that generate bursting in this model can be entirely identified in this range, and this will be demonstrated in the next subsection.

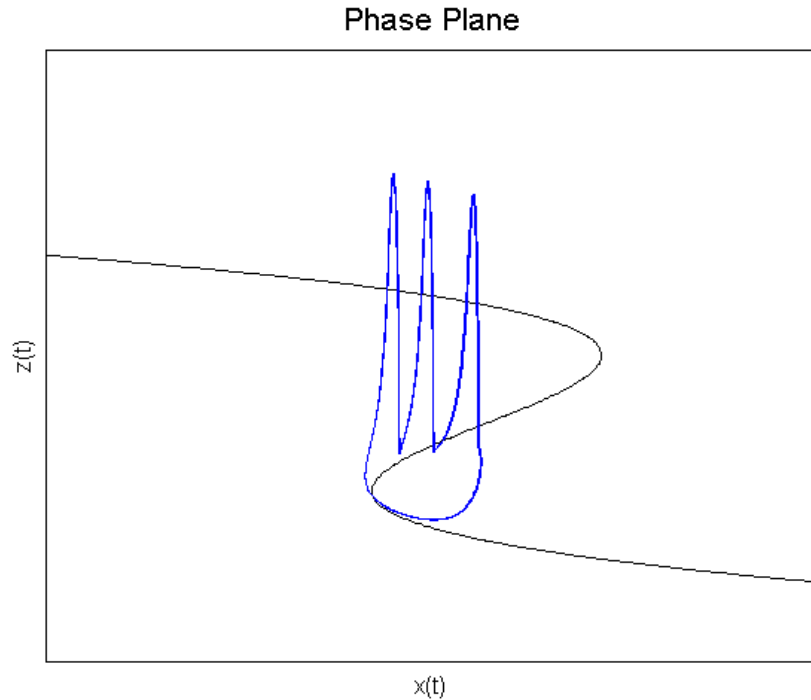


Figure 3.10: Representation of the hysteresis loop in the reduced Hindmarsh-Rose model. The blue line represents the motion of a phase point as w is first increased and then decreased.

3.2.3 Hysteresis in the Reduced Model

In the previous subsection, we swept across a range of values for the parameter w and located several bifurcations in the dynamics of the reduced Hindmarsh-Rose model. Here we will show how bursting behavior can be interpreted from this reduced model if we imagine tweaking the parameter w slowly and observing how the system reacts. Specifically, we trace the motion of a phase point — an imaginary point that travels along trajectories — as it is subject to a bifurcating system.

If we begin by picking w in the leftmost region, say at $w = -0.5$, our phase point will travel on the stable limit cycle (refer to Fig. 3.9). As we increase w , the phase point will remain on the limit cycle, even as the saddle-node bifurcation is encountered, creating two additional fixed points. The phase point on the limit cycle corresponds to the spiking region of the bursting trajectory.

As we increase w further, however, we encounter the leftmost homoclinic bifurcation, and the limit cycle is destabilized. From our previous analysis, the phase point will jump down to the branch of stable fixed points. We begin to decrease w , now. Since the phase point is on a branch of stable fixed points, it will remain there as we decrease the parameter. The phase point adhering to these fixed points corresponds to the quiescent region of the bursting trajectory.

Eventually, decreasing w will result in reaching the leftmost saddle-node bifurcation again. This time, the two additional fixed points will be destroyed, and only a single stable structure remains in the system: the stable limit cycle. The phase point jumps upward and rides along the limit cycle again. From here, we increase w and the spiking region of the bursting trajectory begins

again.

This description of the bursting trajectory reveals the importance of the form of the Hindmarsh-Rose equations. We have seen that the y equation, quadratic in x , gives rise to the two additional fixed points and thus to the bistable region that our above description takes much advantage of. The system displays a hysteresis loop about this bistable region: as we increase w through the region we have spiking behavior, yet as we decrease w through the region we have quiescent behavior. The process described above is illustrated in Fig. 3.10.

3.2.4 The Full Model

Our analysis has considered only the reduced, two-dimensional form of the Hindmarsh-Rose model. We claim that the hysteresis loop that we saw in the phase plane is still preserved in the full three-dimensional model. The full model,

$$\begin{cases} \dot{x} = y - ax^3 + bx^2 + I - z, & (3.3a) \\ \dot{y} = c - dx^2 - y, & (3.3b) \\ \dot{z} = r(s(x - x_1) - z), & (3.3c) \end{cases}$$

adds the third variable, the adaptation current z . In our previous analysis, we treated z as varying slowly, and were able to justify imagining z as a parameter. In fact, z can be thought of as slowly modulating the dynamics of the first two equations.

In Fig. 3.11 we have a bursting trajectory for the full model. The trajectory forms a sort of “coffee-cup” shape in phase space. The stacked loops correspond to the rapid spiking regime of the bursting trajectory, while the “handle” of the cup represents the quiescent state between bursts. From these phase space trajectories, we can observe the modulating effect that z has on the x and y variables: z steadily increases during the bursting regime, and upon reaching some maximum value, decreases during the quiescent stage.

This three-dimensional trajectory confirms our conclusions from the reduced model. If we want to take a more quantitative approach, we can construct the Jacobian matrix for the system,

$$J(\bar{x}, \bar{y}, \bar{z}) = \begin{bmatrix} -3a\bar{x}^2 + 2b\bar{x} & 1 & -1 \\ -2d\bar{x} & -1 & 0 \\ rs & 0 & -r \end{bmatrix}$$

to determine stability of the system’s fixed points. Note that the Jacobian matrix is written entirely in terms of the x -coordinate of the fixed points, \bar{x} , and the parameters. We can find the fixed points by eliminating y and z from the nullclines:

$$0 = a\bar{x}^3 + (d - b)\bar{x}^2 + s\bar{x} - (I + c + sx_1)$$

Note that this approach will be much more complicated than our reduction approach. In particular, the solutions to this cubic are not simply written, and evaluating the eigenvalues of this 3×3 Jacobian matrix at these values is no trivial matter.

Alternative methods of determining local stability without explicitly computing eigenvalues have been proposed. In particular, the Routh-Hurwitz criteria provide a way to determine when a fixed point is stable by comparing the coefficients of the characteristic polynomial of the Jacobian

matrix [2]. Though not applied here, the method is relatively straightforward for 3×3 matrices, and could be applied for various \bar{x} to determine when fixed points are stable.

This brief consideration of the full model should inspire an appreciation for our earlier reductionist approach, and the trajectories shown in Fig. 3.11 confirm our conclusions.

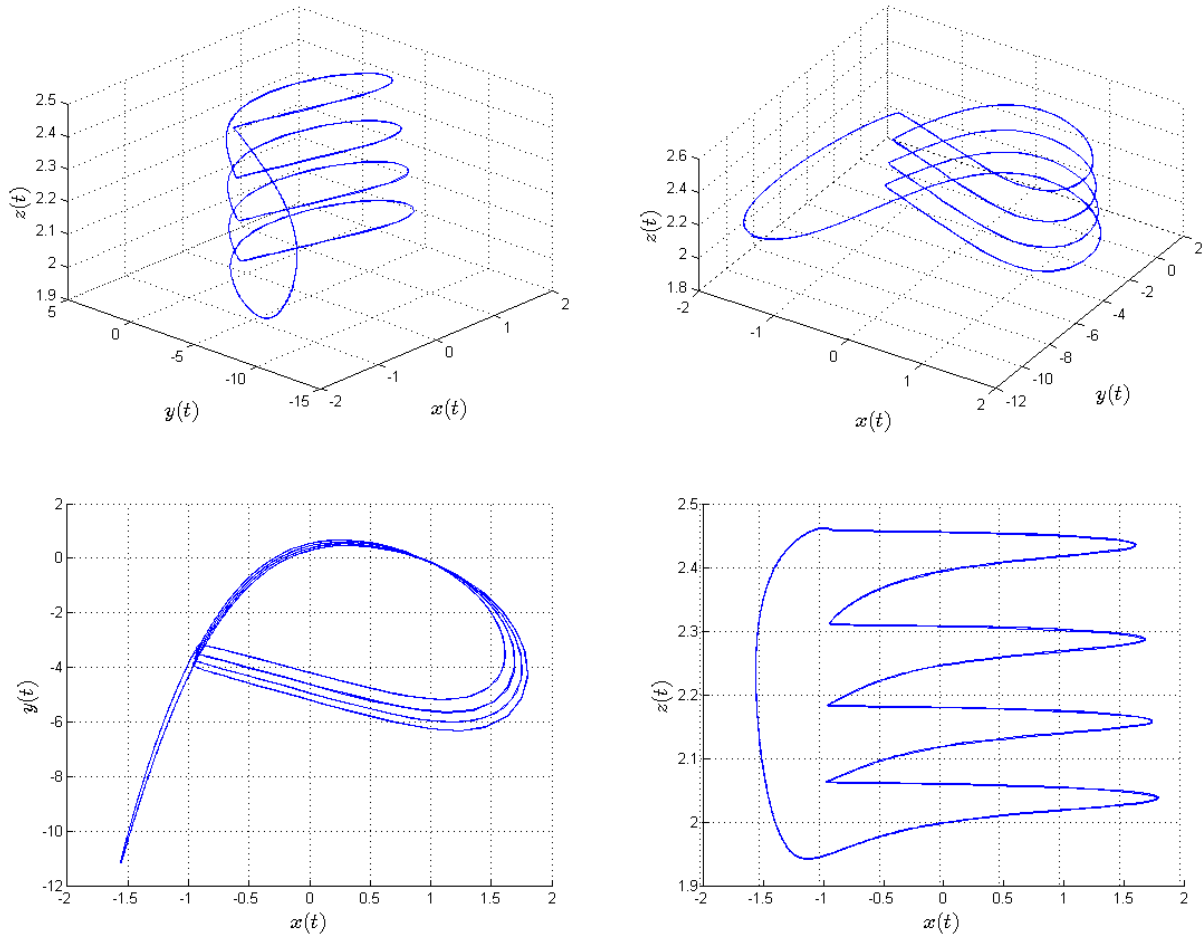


Figure 3.11: Trajectories for the three-dimensional Hindmarsh-Rose system in phase space. Note that the projection onto the $x - y$ plane (lower left) resembles the limit cycle observed in the reduced model.

3.3 Future Work

In this section we briefly point to two interesting directions in which a study of this model might proceed: an analysis of the chaotic dynamics of the model or an attempt to couple multiple Hindmarsh-Rose neurons together.

3.3.1 Chaotic Dynamics

An interesting Hindmarsh-Rose trajectory is shown in Fig 3.12. Note that the bursts have variable numbers of spikes. This is an example of chaos in the dynamical system. Chaos is best thought of as a sensitive dependence on initial conditions [10]. That is, small changes in initial conditions gives rise to drastic changes in long-term behavior.

Since the full Hindmarsh-Rose model is three-dimensional, chaos is possible. An analysis of the chaotic behavior in this model could include the computation of Poincare sections for the system. Additionally, the chaotic trajectories could be compared to experimentally-measured neural voltage traces. In this way, the physical accuracy of this model could be determined; that is, how is chaos observed in the real nervous system?

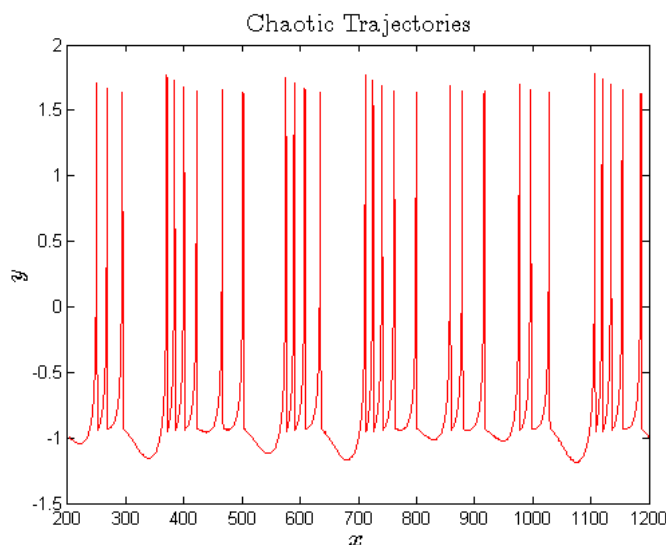


Figure 3.12: Chaos in the Hindmarsh-Rose model. The number of spikes per burst is not constant and effectively impossible to predict.

3.3.2 Coupling

In the 1984 paper introducing the Hindmarsh-Rose model, the authors comment that the model was developed with coupling in mind [9]. In particular, the Hodgkin-Huxley system is too complex to successfully couple two bursting neurons together and understand the behavior. The Hindmarsh-Rose model is much simpler and primarily demonstrates bursting, and so it very suited for coupling.

By coupling, we refer to the adjoining of two Hindmarsh-Rose systems through the addition of

terms to various equations. For instance, we might apply a brute-force sort of coupling whereby we add terms to the membrane voltage equations:

$$\begin{cases} \dot{x}_1 = y_1 - ax_1^3 + bx_1^2 + I - z_1 + \gamma_{12}(x_1 - x_2), & (3.4a) \\ \dot{y}_1 = c - dx_1^2 - y_1, & (3.4b) \\ \dot{z}_1 = r(s(x_1 - x_0) - z_1), & (3.4c) \\ \dot{x}_2 = y_2 - ax_2^3 + bx_2^2 + I - z_2 + \gamma_{21}(x_2 - x_1), & (3.4d) \\ \dot{y}_2 = c - dx_2^2 - y_2, & (3.4e) \\ \dot{z}_2 = r(s(x_2 - x_0) - z_2), & (3.4f) \end{cases}$$

This is an example of linear coupling, where we apply coupling terms of the form used in spring-force equations,

$$\gamma_{ij}(x_i - x_j)$$

in the membrane voltage equations. Note that this results in a six-dimensional system. Additionally, we assumed in Eqns. 3.4 that the parameters are the same for both neurons. These are very strict assumptions, and an analysis of this model would be quite involved and perhaps not very intuitive.

Other methods for coupling neurons have been proposed [12]. Some potential simplifications involve the reduction of our three-dimensional model to a one-dimension phase oscillator model [16]. In this sort of representation, the dynamical system is described as a single equation whose variable represents the phase of the oscillator. Ultimately, information about the amplitude of the oscillator is lost. These models simplify coupling, as two coupled neurons can be described in only two equations as compared to the above six.

Much work has been done in analyzing these one-dimensional phase oscillators. This reduction of a model to a phase oscillator representation is far from trivial. In particular, the reduction involves the computation of a phase resetting function, which describes the effect of an input signal on the phase of a neuron. This function is generally computed numerically, and requires the oscillator to be written in terms of its phase. Future work in this direction would involve the numerical computation of the phase resetting function and its implementation in the reduction of the Hindmarsh-Rose system to a phase oscillator.

Bibliography

- [1] B. Van der Pol. On “relaxation-oscillations”. *The London, Edinburgh, and Dublin Philosophical Magazine and Journal of Science*, 2:978–992, 1926.
- [2] Leah Edelstein-Keshet. *Mathematical Models in Biology*, volume 46 of *Classics in Applied Mathematics*. Society for Industrial and Applied Mathematics, 2005.
- [3] G. Bard Ermentrout and David H. Terman. *Mathematical Foundations of Neuroscience*. Interdisciplinary Applied Mathematics. Springer, 2010.
- [4] Richard FitzHugh. Impulses and physiological states in theoretical models of nerve membrane. *Biophysical Journal*, 1:445–466, 1961.
- [5] Avner Friedman. Introduction to neurons. In A. Borisjuk, G.B. Ermentrout, A. Friedman, and D.H. Terman, editors, *Tutorials in Mathematical Biosciences I*, pages 1–20. Springer, 2005.
- [6] Jean-Marc Ginoux and Christopher Letellier. Van der pol and the history of relaxation oscillations: Toward the emergence of a concept. *Chaos: An Interdisciplinary Journal of Nonlinear Science*, 22, 2012.
- [7] J.L. Hindmarsh and Philip Cornelius. The development of the hindmarsh-rose model for bursting. In Stephen Coombes and Paul C. Bressloff, editors, *Bursting - The Genesis of Rhythm in the Nervous System*. World Scientific, 2005.
- [8] J.L. Hindmarsh and R.M. Rose. A model of the nerve impulse using two first-order differential equations. *Nature*, 296(11):162–164, March 1982.
- [9] J.L. Hindmarsh and R.M. Rose. A model of neuronal bursting using three coupled first order differential equations. *Proceedings of the Royal Society of London*, 221(1222):87–102, March 1984.
- [10] Morris W. Hirsch, Stephen Smale, and Robert L. Devaney. *Differential Equations, Dynamical Systems, and an Introduction to Chaos*. Elsevier, Inc., third edition, 2013.
- [11] A.L. Hodgkin and A.F. Huxley. A quantitative description of membrane current and its application to conduction and excitation in nerve. *The Journal of Physiology*, 117:500–544, 1952.

- [12] Eugene M. Izhikevich. *Dynamical Systems in Neuroscience: The Geometry of Excitability and Bursting*. The MIT Press, Cambridge, Massachusetts, 2007.
- [13] A. Shilnikov and M. Kolomiets. Methods of the qualitative theory for the hindmarsh-rose model: a case study. a tutorial. *International Journal of Bifurcation and Chaos*, 18, 2008.
- [14] Steven H. Strogatz. *Nonlinear Dynamics and Chaos: With Applications to Physics, Biology, Chemistry, and Engineering*. Studies in Nonlinearity. Perseus Books, 1994.
- [15] David Terman. An introduction to dynamical systems and neuronal dynamics. In A. Borisyuk, G.B. Ermentrout, A. Friedman, and D.H. Terman, editors, *Tutorials in Mathematical Biosciences I*, pages 21–68. Springer, 2005.
- [16] Arthur T. Winfree. *The Geometry of Biological Time*, volume 8 of *Biomathematics*. Springer-Verlag, 1980.

STANLEY L. TUZNIK ACADEMIC VITA

slt5237@psu.edu • 1610 West 39th St., Erie, PA 16509 • (814) 464-7828

OBJECTIVE

Obtain admission into a graduate program in applied mathematics. Research interests involve the application of rigorous mathematical and computational methods to complex physical dynamical systems. Of particular interest are oscillatory neural systems.

EDUCATION

Pennsylvania State University, the Behrend College **Expected May 2015**

- B.S. in Applied Mathematics **GPA: 3.88**
- B.S. in Physics

PROFESSIONAL EXPERIENCE

Student Researcher in Mathematics, Penn State **2014 — Present**

- *Neurodynamics Research Project* — Investigated the behavior of bursting oscillations in neurons through use of traditional dynamical systems techniques. Visualizations and solutions were obtained through MATLAB.
- *Honors Thesis* — Studied the Hindmarsh-Rose model for single-neuron bursting. Thesis reviews earlier models for bursting and discusses an attempt to couple two Hindmarsh-Rose neurons through reduction to equivalent phased oscillator models. Work will be presented at several conferences in the spring of 2015.

Student Researcher in Physics, Penn State **2011 — 2014**

- *Computational Solid Modeling* — Conducted computational research involving the formation of experimentally-accurate models of amorphous silicon using C++. Work involved debugging code as well as writing algorithms to compute radial distribution functions, energies, and forces for large systems of atoms.
- *LSC Lab* — Worked on designing experiments to optimize luminescent solar concentrators through the application of metal enhanced fluorescence from metal nanoparticles.

Physics Intern, FMC Technologies **2013 — Present**

- *Ultrasonic Engineering* — Worked alongside engineers in a research-and-development environment to optimize ultrasonic transducer technology for measurement applications in oil and gas industry.

Education, Penn State **2011 — Present**

- *Mathematics and Physics Tutor* — Met with students outside of class to explain, reinforce, and supplement concepts taught in introductory physics and mathematics courses.

- *Physics Teacher's Assistant* — Assisted professors in explaining and demonstrating physical and mathematical concepts taught during lecture in introductory physics courses on mechanics and electricity and magnetism. Duties included regular grading of assignments and quizzes.

Local Arts, Erie, PA

2009 — Present

- *Band Founder, Manager, and Member* — Organized events, coordinated schedules, managed funds, co-wrote songs, and performed with a local musical ensemble at both paid and charity events.

PRESENTATIONS

- *The Neurodynamics of Bursting Oscillations in the Hindmarsh-Rose Model*
 - Joint Mathematics Meeting, San Antonio, TX. January 2015.
 - Undergraduate Mathematics Research Conference, Youngstown State University, Youngstown, OH. February 2015.
 - Sigma Xi Undergraduate Research Conference, Penn State Behrend, Erie, PA. April 2015.
- *Some Issues Regarding Quaternion Calculus*
 - Sigma Xi Undergraduate Research Conference, Penn State Behrend, Erie, PA. April 2015.

SKILLS

- *Programming* — Working knowledge of C++, Scientific Python, Maple, and MATLAB.
- *Other* – Good knowledge of the L^AT_EX typesetting package.

HONORS

- Academic Excellence Award in Physics 2015, Penn State Behrend
- Academic Excellence Award in Mathematics 2015, Penn State Behrend
- Mathematics Scholarship Competition Award 2015, Penn State Behrend
- School of Science Scholarship 2012-2013, Penn State Behrend
- Mathematics Research Scholarship, Penn State Behrend
- Schreyer Honors Scholar, Penn State University
- Penn State Behrend Writing Award 2014 for research paper titled *Experimental Observation of Quantum-Mechanical Wave-Particle Duality of Light through Slit Experiments*
- Physics Teacher's Assistant of the Year Award, 2011, Penn State Behrend
- Pi Mu Epsilon, National Mathematics Honors Society
- Sigma Pi Sigma, National Physics Honors Society
- Physics and Astronomy Club President, 2013-2015, Penn State Behrend
- SIAM Student Member
- Dean's List, 2010-2015, Penn State Behrend
- Chancellor's Scholarship 2010-2014, Penn State Behrend